



## Development of Eco-Friendly Modified Natural and Synthetic Nanozeolites, for Urea Efficient Delivery to Vegetable Plants with Reducing Nitrogen Losses to Environment



Fatma E. Ibrahim <sup>a</sup>, Mohamed I.D. Helal <sup>a</sup>, Noha H. Abdelkader <sup>a</sup>, Mohamded A. Mohamady Hussein <sup>b\*\*</sup>, Ibrahim M. El-Sherbiny <sup>c\*</sup>,

<sup>a</sup> Soil Sciences Department, Faculty of Agriculture, Cairo University, Giza 12613, Egypt

<sup>b</sup> Department of Pharmacology, Medical Research and Clinical Studies Institute, National Research Centre, 33 El Bohouth St., Dokki, Giza 12622, Egypt

<sup>c</sup> Zewail City of Science and Technology, 6th October City, 12578, Giza, Egypt

### Abstract

A commercial urea fertilizer typically exhibits a fast-release profile with the drawback of soil loss, leading to environmental hazards and limiting its application in plant cultivation. Previous efforts have focused on nanoparticulating urea to overcome these challenges and broaden its usage in agriculture while ensuring environmental safety, including humans, animals, and water, and preventing nitrate pollution. While many studies concentrate on synthetic nano zeolite (SNZ) as nanocarriers for plant fertilizers, this current study aims to enhance the properties of natural zeolites to increase their loading capacity for urea through physical preparation, followed by thermal or chemical modifications (physically-prepared NZ, PNZ). The study proposes a simple physical emulsion technique to adsorb urea molecules onto the surface of the as-prepared physically modified nano zeolite (PNZ) to create urea-PNZ (U-PNZ) for the soil's slow and sustained release of nitrogen. Chemical and morphological characterization of the produced U-PNZ was conducted using DLS (hydrodynamic diameter and  $\zeta$ -potential), FTIR, XRD, SEM, and TEM. Confirmation of urea encapsulation in PNZ indicated an increase in DLS size from 87.0 nm in PNZ to 111.0 nm in U-PNZ, accompanied by a decrease in  $\zeta$ -potential. The study observed enhanced adsorption properties of urea to PNZ compared to non-treated Z (Z). Release profiles of commercial urea, Z, and the developed NZ systems were recorded, demonstrating that both NZ systems (U-PNZ and U-SNZ) exhibited slower and controlled nitrogen release than commercial urea and Z. A pot experiment was conducted to showcase the efficiency of NZ systems loaded with urea on lettuce, evaluating nitrogen, protein content, and growth behavior. Results indicated higher growth rate parameters in lettuce treated with U-PNZ and U-SNZ compared to free urea or U-loaded Z. This study suggests that PNZ could serve as a promising platform for efficient urea adsorption with controlled release in the soil, presenting a better profile than commercial urea or Z. Further studies are required to refine the efficiency of PNZ, particularly in enhancing the growth rate of vegetable plants induced by SNZ or other materials.

**Keywords:** Natural Nanozeolites, Synthetic Nanozeolites, Urea, Reducing Nitrogen Losses, Urea Slow and Sustained Release, Growth Rate Parameters

### 1. Introduction

The agricultural sector faces a growing demand for agrochemicals to boost soil fertility and productivity [1]. Nitrogen (N) plays a pivotal role in plant growth, crucial for carbon metabolism and protein synthesis [2]. The fertilizer industry consumes 60 to 75% of global nitrogen [3], with urea being the predominant traditional fertilizer due to its high N content and cost-effectiveness [4]. However, substantial losses (40-60%) of applied urea occur through denitrification, volatilization, leaching, and runoff, particularly in the nitrate form [5]. These losses have significant economic and environmental consequences [6], leading to the development of innovative nitrogen agrochemicals with targeted delivery.

Various approaches have been explored in this context. Initially, soil amendments such as biochar [7], biomass [8,9], and clay minerals [10] have been employed as carriers, releasing loaded fertilizers slowly and in a sustained pattern. Coating approaches [11] involving materials like polymers [12] and biodegradable polymer blends [13] have also been developed to enable controlled-release fertilizers. Additionally, engineered nanomaterials have enhanced targeted delivery, ensuring more controllable release patterns for maximum efficiency and sustained soil health. Examples include nano clay-based fertilizers

\*Corresponding author e-mail: [almohammadeymr2023@gmail.com](mailto:almohammadeymr2023@gmail.com); (Mohamed Hussein).

Receive Date: 06 June 2024, Revise Date: 11 August 2024, Accept Date: 15 August 2024

DOI: 10.21608/ejchem.2024.288791.9815

©2025 National Information and Documentation Center (NIDOC)

[14], silica nanoparticles [15], hydroxyapatite nano fertilizers [16], chitosan-based nanoparticles [17], inorganic-organic hybrid nanomaterials [18,19,20], and nanocomposites designed for the smart release of fertilizers [21].

Considerable progress has been achieved in exploring innovative porous nanomaterials, with zeolite [22] emerging as an ideal candidate for a carrier system in fertilizer delivery. Zeolites are crystalline aluminosilicate materials composed of tetrahedrons of SiO<sub>4</sub> and AlO<sub>4</sub>, forming three-dimensional secondary building units (SBU) when various combinations of primary building units (PBU) combine with oxygen, as defined by the International Mineralogical Association [23]. The unique structure of zeolites includes internal pores and channels ranging from 0.3 to 3 nm, with an inner surface extending several hundred square meters per gram. Various parameters, such as the presence of active sites, negatively charged aluminum units, shape selectivity, chemical composition, Si/Al ratio, and the presence of different metal cations in the crystal structure, contribute to their versatility. As a result, zeolites find applications in numerous chemical industries, including oxidation, reduction, hydrolysis, dehydration, cracking, alkylation, isomerization, molecular sieves, hydration, sorption, adsorption, ion exchange, and catalysis [24].

2. Zeolites have diverse applications across various fields, including construction and building materials, water purification, wastewater treatment, environmental cleanup, consumer goods, medicine, and technical applications [25], [26], [27]. They are also utilized in heavy metal removal [28], energy refinery and storage [29], molecular sieves [30], biomass transformation [31,32], animal production and human pathogenesis [33], the food industry [34, 35], and food production [36].

In the agricultural sector, zeolites find diverse applications, contributing to soil enhancement in agronomy, serving as dietary supplements for animals, acting as insecticides and pesticides for plant protection, being utilized as hydroponic (geoponic) substrates for growing plants on space missions and playing a role in dust applications in organic farming for integrated pest management (IPM) procedures [37]. Zeolites have various applications in agriculture and commerce, including odor control, mycotoxin control, use in horticultural nurseries and greenhouses, soil amendment, reclamation, revegetation, and the development of slow-release fertilizers [39]. Additionally, zeolites have the potential to enhance water retention in sandy soils and improve porosity in clay soils [40]. They have been successfully employed as carriers of soil conditioners, organic manure, and nutrients [41] [42].

Modifying natural zeolite is a widely recommended practice to alter the surface charge and characteristics, enhancing the selectivity for removing or adsorbing ions [43], [44]. Reports indicate that 3.1 million tons of zeolite were consumed overall, with 18% sourced from natural deposits and the remainder from synthetic sources such as A, X, and Y. However, the cost of synthetic nanozeolites (SNZ) and logistical limitations pose significant obstacles. There is now a greater focus on obtaining low-cost synthetic zeolite with numerous advantages over its natural counterparts [45]. Synthesis parameters for SNZ can be adjusted for specific purposes [46]. Other studies demonstrate a significant capacity of SNZ in the adsorption of heavy metal ions [47]. Modified synthetic zeolite-4A reduced the equilibrium time required for groundwater treatment by 29–50% efficiency [48].

Current research studies have focused extensively on surface modifications of natural zeolite to enhance its applications. Both physical and chemical changes are employed in natural clinoptilolite to improve its sorption and ion exchange capabilities [49], [50,51]. Combined modifications involving alkali, acid, and salt composites are also explored [52], [53]. Modifying natural zeolites with NaNO<sub>3</sub> and heating at 400°C increased the removal efficiency of ammonium by 39.88% [54], while ultrasound-modified zeolite enhanced removal efficiency by approximately 30% [55]. Advanced organic matter recovery has been achieved using modified natural zeolite [56]. Modified natural zeolite has shown increased absorption capacity for Hg<sup>2+</sup> [57,58].

Regarding the high capacity of natural and synthetic nanozeolites to enhance the efficiency of fertilizers, ongoing research is addressing challenges and exploring modifications [60]. The current work focuses explicitly on utilizing natural zeolites at ultra-small sizes or nanoscales to enhance their adsorption capability for fertilizers, particularly urea. To the best of our knowledge, this study is the first to systematically modify natural zeolites using multiple adjusted parameters to create efficient modified PNZ comparable to SNZ, with optimal characteristics in terms of stability, nanoscale properties, surface area, urea loading capacity, sustained and slow release, and promotion of lettuce growth efficiency. This research employs various enhancement methods, including thermal and chemical modifications, to transform natural zeolite (Z) into more uniform nanoscale structures, referred to as nanozeolites (NZ), with the potential to adsorb and encapsulate urea molecules more efficiently. Physically prepared natural nanozeolites (PNZ) were synthesized and then subjected to thermal or chemical modifications under various parameters to serve as promising urea (U) carriers in agricultural applications. The ultimate goal is to refine natural zeolites to the point where they can replace synthetic ones, aiming to achieve improvements that qualify natural zeolite as synthetic NZ (SNZ). FTIR was employed to confirm the chemical composition of both PNZ and SNZ. Morphology and elemental compositions were studied using TEM and SEM-EDX. Encapsulation efficiency for urea (U) was assessed in various modified PNZ and SNZ. DLS measurements, including hydrodynamic diameters and zeta potential, were recorded. Urea release patterns from the developed U-PNZ were investigated and compared to commercial urea and U-SNZ.

Additionally, compared to commercial U and U-loaded Z, a pot experiment was designed to demonstrate the efficiency of U-loaded NZ systems on lettuce, assessing nitrogen and protein content and growth behavior.

## 2. Materials and Methods

### 2.1 Materials:

The natural zeolite (Z) from Yemen was provided by Alix-Zeolite Company for zeolite in Giza, Egypt. Aluminum, sodium hydroxide (NaOH), and di-hydrated sodium, potassium and calcium chloride used in this research were purchased from Loba Chemie (Mumbai, India). Commercial silicate solution and commercial urea were purchased from a local chemicals store market in Giza City, Egypt.

### 2.2. Preparation of zeolites (Z) and nanozeolites (NZ)

Natural zeolite (Z):

Natural zeolite was washed several times using DI water, air-dried, and sieved without extra purification, where it was coded as Z.

Physically-prepared nanozeolite (PNZ):

It was fabricated by size reduction of natural zeolite using a top-down approach through a high-energy ball milling grinder (Model: PH-BML911) at the Soil Science Department, Faculty of Agriculture, Cairo University. Spheres of stainless-steel balls were used for grinding the media. The sample-to-stainless steel ball ratio was adjusted to (1:20). Briefly, 15g of natural zeolite was placed in each of the 4 slender and rotated at a speed of 1900 rpm for 30 h, divided into 6 days' work. Then, it is sieved and kept for further study and analysis.

Modified Z and PNZ:

The modification of Z and PNZ was conducted via thermal (T) and chemical (C) methods on their surfaces to maximize the capacity of loaded urea into the zeolite structure, as shown in **Table 3**. Thermal modification includes using different temperatures and durations as described [61,62]. Chemical modifications are also conducted using a 2M solution of NaCl, KCl, or CaCl<sub>2</sub> under control parameters as described [63] [64].

Synthetic nanozeolite (SNZ):

SNZ was fabricated using a bottom-up approach by incorporating the simple hydrothermal liquid crystallization technique and microwave method to yield better results in less time [65] [66]. A microwave model (Milestone, ETHOS-130127) with easy control software and HPR1000/105 high-pressure segmented rotor (50-60HZ/220watt) at the research park (CURP), Cairo University, was utilized. SNZ was prepared using a facile, low-cost, and environmentally friendly approach [67] [68] [69]; the aging period and crystallization temperature were studied [70] [71] [72] throughout four phases to achieve the appropriate structure of SNZ for the current study, as displayed in **Table 2**. In brief, a sodium aluminate solution was obtained by mixing 30% (w/v) sodium hydroxide aqueous solution with 90 g of aluminum powder. Then, 100 ml of commercial sodium silicate solution was added dropwise to the previously prepared sodium aluminate solution under vigorous stirring and lifting for 1 hour agitation at room temperature. The mixture was kept for aging periods of one day or 30 days at room temperature and then transferred to a microwave vessel at different crystallization temperatures of 90°C or 110°C for 4 hours. The four obtained SNZ samples were filtered and washed until pH reached 9 and dried in an oven at 80°C to be kept for further study and analysis.

### 2.3. Urea-loaded Z and NZ

Commercial urea was loaded into all previously prepared Z and NZ, either SNZ or PNZ, using a simple physical emulsion technique with the assistance of a water bath at pH (6.5 – 7.5), shaking velocity (150 c/m), and temperature (35°C). Additionally, the preparation process included loading urea at three different equilibrium times, as shown in **Table 3**.

#### 2.4. Physicochemical characterizations of Z, PNZ and SNZ

The main physical properties such as color, moisture content, water absorption capacity (WAC%), pH, electrical conductivity (EC) and bulk density of Z, PNZ and SNZ were evaluated [73]. The color of the samples was determined by the naked eye. The percentage of moisture content or internal water was calculated after drying the pre-weighed samples (W2) in the oven at 105°C from dry weight (W1) according to the equation below [74]. WAC% or swelling ratio was calculated after soaking the pre-weighed samples (W1) in water for a while till saturation, then filtrated and re-weighed (W2), where the percentage of water absorption capacity according to the equation below [75]. PH (acidity and alkalinity levels) and EC were determined in the suspension ratio of samples to water (1: 2.5) using a pH meter (Accumet AR.20, Fisher Scientific, Waltham, MA, USA) and EC meter (JENWAY, London, UK, 4510), respectively [76]. The samples' bulk density (g/cm<sup>3</sup>) was determined using the dry weight ratio to the volume [74].

$$\text{WAC \%} = \frac{\text{Wet weight (W2)} - \text{Dry weight (W1)}}{\text{Dry weight (W1)}} \times 100$$

The crystalline structure of Z, PNZ, and SNZ was determined using XRD (Philips Xpert-PRO-MPD- Netherlands) at 30 mA and 40 kV, with a Cu Anode. The shape and size of zeolites were determined using a transmission electron microscope (TEM, Model JEM-2100 electron microscope). The morphological shape of zeolites was studied using a scanning electron microscope (SEM) at a magnification of 120,000 × and an acceleration voltage of 200 kV. Additionally, EDX was used to identify ratios of the elemental composition of Z, PNZ, and SNZ (Model ESEM - FEI Quanta 250 FEG - Netherlands). The average hydrodynamic diameters of all samples before and after loading U were determined, and Zeta potential was recorded as well with DLS to determine the change in the surface charges after loading the U. The most crucial property of zeolites in the current study is the specific surface area, which was characterized using (BET) by a surface area analyzer (Autosorb-1, Quantachrome Instruments, Boynton Beach, FL, USA). N<sub>2</sub> adsorption at 196.15°C was performed, and the prepared sample was degassed at 250°C for 2 hours under a reduced pressure of 33.5 atm before examination. The total surface area was calculated using the multipoint BET equation in the software. Functional groups were identified in all samples using Fourier-transform infrared spectroscopy (FTIR-460 plus spectrometer, JASCO, Japan) in a range of wavelengths from 4000 to 400 cm<sup>-1</sup>. The fingerprints of all samples were studied using Raman spectroscopy (Horiba lab RAM HR evolution visible single spectrometer).

#### 2.5. Encapsulation efficiency

Ultimately, the urea-loaded Z and NZ were filtered, left to dry in the open air, and then stored to determine the total nitrogen content, different characteristics, and release studies. Entire nitrogen content was determined using ammonia distillation (Kjeldahl unit Protein-Nitrogen Distiller, RAYPA, Barcelona, Spain) after complete digestion of samples according to [77]. Urea-loaded samples were expressed with total nitrogen per cent from the following equation: Nitrogen% = (1.4 × V × N) / (W), where V is the volume of acid used, N is the normality of acid, and W is the weight of the substance. The highest nitrogen percentage was selected in the release and growth studies in the following three samples (CZ-2, TPNZ-1, and SNZ-1) for 1 hour, as shown in **Table 3**.

#### 2.6. Urea release studies

The release study was performed in a liquid medium (water) and a solid medium (washed sand). Water release behavior was measured by weighing 0.2g samples in triplicates (free urea U, U-Z, U-PNZ, or U-SNZ) in a 50 mL Falcon tube. Gradually, 20 ml DI water was added. Water was collected for nitrogen analysis at predetermined times over 20 days. The total nitrogen

content was determined in the collected water using the Kjeldahl unit, as described in [77]. For the urea release in washed sand, glass columns (20cm height and 1.5cm width) were filled with 50g of washed soil. Then, 0.2g sample triplicates (free urea U, U-Z, U-PNZ, or U-SNZ) were buried in the topsoil columns with the addition of 17mL of water to achieve a soil saturation of 20-25%. Subsequently, the same amount of water was added slowly, and leachates were collected from the end neck of columns at predetermined times over 20 days. As mentioned previously, the total nitrogen content was determined in the collected leachates using the Kjeldahl unit.

### 2.7. Growth study

A pot experiment assessed the efficiency of urea-loaded Z and NZ compared with free urea. The study was performed in a standard greenhouse in Giza, Egypt. Seedlings were grown in December in pots containing 5 kg of silty loam soil, and the plants were collected in February. Table 3 shows the physical and chemical properties of the experimental soil and irrigation water [74]. Free urea (U) and U-loaded samples (U-Z, U-PNZ, or U-SNZ) were added at two rates of addition (100% and 50%) above the recommended dose of free urea. All pots were represented in triplicates.

Additionally, other farming procedures were performed according to the recommendations of the Ministry of Agriculture in Egypt [78] [79]. Surface irrigation was added to pots at 55-65% of the equivalent field capacity of the experimental soil. At the end of the experiment, the number of leaves, leaf and root length, and fresh and dry weight were estimated. Furthermore, the total nitrogen content in lettuce was determined using the Kjeldahl unit [74]. In contrast, the complete protein content was assessed using the following equation: Total protein content (%) = Total nitrogen (%) × Protein factor [80][81].

### 2.8. Statistical analysis

The results were analyzed using GraphPad Prism 8.0.2 software, GraphPad Software. The results were expressed as means ± SD, where statistical significance was evaluated using one-way ANOVA (\* p < 0.05).

## 3. Results and discussion

### 3.1. Synthesis of chemically and thermally modified zeolite and NZ

The surface of zeolite and/or NZ was activated through thermal and chemical methods to enhance the efficiency of the specific surface area and achieve the best comparison with the third type of NZ chemically synthesized. Surface activation via thermal or chemical modification is a widely recommended practice for altering zeolite and NZ's surface charge and characteristics as carriers, thereby enhancing their adsorption or desorption capabilities. Thermal modification involves utilizing different degrees of thermal activation to increase the effective surface area of zeolite. This process depends on the evaporation and removal of excess water molecules from the voids, facilitating the entry of the fertilizer element. In chemical modifications, the ion exchange properties of zeolite were exploited through the reaction of zeolite or NZ with NaCl, KCl, and CaCl<sub>2</sub> at adjusted parameters to enhance the reaction.

Moreover, a significant portion of commercially available zeolites can be produced synthetically. In this context, we prepared synthetic NZ (SNZ) through a chemical synthesis approach. This involved a bottom-up process, combining simple hydrothermal liquid crystallization and microwave methods. The hydrothermal and microwave processes were employed to produce SNZ efficiently in a relatively short time. Various parameters and protocols were adjusted throughout this approach, resulting in four phases of the produced NZ. This comprehensive approach aimed to identify the most suitable phase in terms of cost-effectiveness, ease of implementation, and eco-friendliness.

### 3.2. Physical properties of the Z, PNZ and SNZ.

The physical properties of Z, PNZ, and SNZ, including color, moisture content %, water absorption capacity (WAC%), pH, electrical capacity (EC), and bulk density, were evaluated and are presented in **Table 1**. The color was determined by the

naked eye, with Z appearing green, PNZ in green light, and SNZ as a white powder. Moisture content was found to be 9%, 12%, and 14.5% in Z, PNZ, and SNZ, respectively. WAC% values were recorded as 23.67%, 37.89%, and 44.83% for Z, PNZ, and SNZ, respectively. The increase in WAC% with decreasing particle size indicated that the more porous structures of PNZ and SNZ, attributed to their high porosity and surface area, allowed them to retain more water than Z. The pH levels were measured at 9.5 for Z, indicating a slight tendency towards alkalinity due to surface OH groups. In contrast, PNZ and SNZ showed pH values of 8.6 and 8.2, respectively. EC values were determined as 0.21, 0.15, and 0.12 dS/m in Z, PNZ, and SNZ, respectively. EC depends on increased broken edges and active sites, influenced by the Si/Al ratio and acid-base properties. Bulk density values were evaluated at 0.82, 0.68, and 0.55 g/cm<sup>3</sup> in Z, PNZ, and SNZ, respectively. Notably, bulk density tends to be lower in materials with smaller particles and higher porosity.

**Table 1** The main physical properties of the Z, PNZ and SNZ1

Properties	Z	PNZ	SNZ1
Color	green	green light	white
Moisture content %	9	12	14.5
WAC %	23.67	37.89	44.83
pH (1: 2.5)	9.2	8.6	8.2
EC (dS/m)	0.21	0.15	0.12
Bulk density (g/cm <sup>3</sup> )	0.82	0.68	0.55

### 3.3. XRD analysis

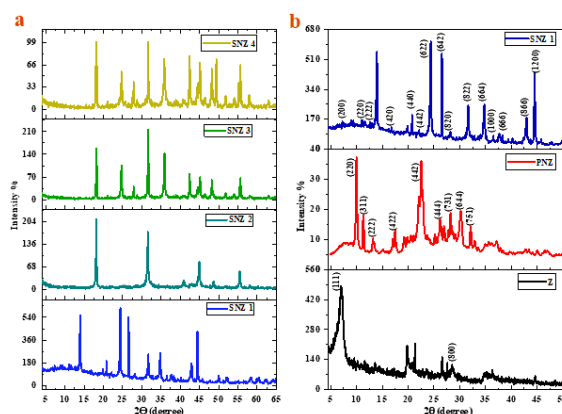
Synthetic nanozeolite (SNZ) was initially prepared under various parameters, resulting in SNZ-1, SNZ-2, SNZ-3, and SNZ-4. These four samples were characterized using XRD, as illustrated in **Fig.1** and **Table 2**. The comparison of the four samples based on XRD analysis was conducted in terms of yield % to identify the purest crystalline zeolite, A. Table 1 indicates that the yield was enhanced by increasing the aging time to 30 days, consistent with findings in previous studies [82] [83] [84]. Additionally, the yield % of SNZ showed improvement with an increase in the crystallization temperature from 90°C to 110°C. In this study, the hydrothermal-assisted microwave process demonstrated a higher yield of crystallinity in a short 4-hour period compared to the traditional hydrothermal technique, which typically requires 8 hours [85] [86] [87] [88]. It has been reported that microwave treatment over a shorter period is preferred to avoid aggregation and the formation of large particle sizes, as longer exposure times can lead to these undesired effects [89] [90].

The XRD patterns of the SNZ-1 sample revealed prominent peaks at 200, 220, 222, 420, 440, 442, 622, 642, 820, 822, 664, 1000, 666, 866, and 1200, corresponding to 7.2°, 10.6°, 12.6°, 16.5°, 20.5°, 21.9°, 24.3°, 27.1°, 29.1°, 30.9°, 34.5°, 36.5°, 38.1°, 42.9°, and 44.3°, respectively. As indicated in **Table 2**, the parameters and conditions used to prepare SNZ-1 were favored, resulting in a 97% crystalline yield. Moreover, SNZ-1 matched the standard zeolite-A (JCPDS Cards Code 01-089-8015), displaying the distinctive structure of type LTA (Linde Type A) characterized by the formula [Na<sub>94.75</sub>(Al<sub>96</sub>Si<sub>96</sub>O<sub>384</sub>)(H<sub>2</sub>O)<sub>39.17</sub>] [91,92,93,94,95]. Consequently, SNZ-1 was chosen as the representative for SNZ for further studies in this work and was coded SNZ [96] [97].

The XRD patterns of Z and PNZ were investigated and indexed, as illustrated in **Fig. 1**. The prominent diffraction peaks of Z were assigned at 111 and 800, corresponding to 6.79° and 28.53°, respectively. For PNZ, the main diffraction peaks were 220, 311, 222, 422, 442, 444, 731, 644, and 752, corresponding to 9.85°, 11.32°, 13.25°, 17.48°, 22.50°, 25.78°, 28.25°, 30.18°, and 32.29°, respectively. Additionally, no additional diffraction peaks were detected, and both Z and PNZ matched with the standard type zeolite (JCPDS card code 01-073-2310).

**Table 2** Crystalline yield % of SNZ samples according to the applied parameters (aging time, temperature and microwave time) throughout their synthesis.

SNZ Code	JCPDS Code No.	Aging time (days)	Crystallization temperature °C	Microwave time	Yield %
SNZ-1	01-089-8015	30	110	4h	97
SNZ-2	01-089-9099	30	90	4h	93
SNZ-3	00-052-0145	1	110	4h	70
SNZ-4	01-089-9098	1	90	4h	42

**Fig. 1** – XRD patterns for a) the 4 synthetic nanozeolites (SNZ); SNZ-1, SNZ-2, SNZ-3 and SNZ-4, and b) Z, PNZ and SNZ-1

### 3.4. Urea loading Efficiency% (LE %) of the treated Z and PNZ and the prepared SNZ 1

Samples Z and PNZ underwent thermal and chemical modifications as described above and in Table 3. Z was thermally treated and coded according to the conditions, resulting in TZ-1, TZ-2, and TZ-3. Z was also chemically treated using NaCl, KCl, and CaCl<sub>2</sub> and coded as CZ-1, CZ-2, and CZ-3. Similarly, PNZ obtained PNZ-1, PNZ-2, PNZ-3, PNZ-4, PNZ-5, and PNZ-6.

The loading efficiency (LE%) of treatments was expressed based on the obtained total nitrogen content, as shown in **Table 3** and **Fig. 2**. All samples, including Z, modified Z, PNZ, changed PNZ, and SNZ, were incubated with urea (U) at three different times (1, 24, and 72 hours) to allow for loading the U through the porous structured samples. The LE% was then recorded after the specified times. It was observed that the LE% of Z was enhanced when treated chemically and thermally. The highest LE% in thermally modified Z (TZ) was recorded at 15.40% and 14.63% in TZ-1 and TZ-3 after 24 hours, respectively, and 8.85% in TZ-2 after 1 hour. In the case of chemical modification, the highest LE% was recorded at 15.59% in CZ-2 after 1 hour, 14.43% in CZ-3 after 24 hours, and 8.85% in CZ-1 after 1 hour. CZ-2, with the highest LE% of 15.59% after 1 hour, was selected as a representative sample of Z for further studies.

On the other hand, it was observed that the loading efficiency (LE%) of PNZ was enhanced when subjected to thermal modifications, with the highest amount recorded at 16.94%, 15.40%, and 13.09% in TPNZ-1, TPNZ-3, and TPNZ-2 after 1 hour, respectively. In the case of chemical modifications, the highest percentage was 15.51% in CPNZ-2 after 1 hour, 15.21%

in CPNZ-3 after 72 hours, and 13.47% in CPNZ-1 after 24 hours. TPNZ-1, with the highest LE% of 16.94% after 1 hour, was selected as a representative PNZ sample for the rest of the study.

A comparison between the LE% of both Z and PNZ before and after thermal/chemical modifications revealed that modifications (thermal and chemical) produced different results but resulted in higher values than those of non-modified samples. The modification treatments significantly improved the porous structure of Z and PNZ by enhancing their ion exchange capacity to adsorb urea molecules. For SNZ, the highest LE% was achieved after 1 hour with 22.33%.

**Table 3** Loading efficiency % of all samples (Z, modified Z, PNZ, modified PNZ and SNZ) after 3 different times.

No.	Code	Treatments	LE (%)		
			1h	24h	72h
1	Z	None	8.08	10.39	10.59
2	TZ-1	100°C/24h	13.47	15.40	13.28
3	TZ-2	225°C/3h	8.85	7.70	7.31
4	TZ-3	400°C/3h	13.47	14.63	10.59
5	CZ-1	NaCl	8.85	8.47	7.89
6	CZ-2	KCl	15.59	11.55	10.39
7	CZ-3	CaCl <sub>2</sub>	12.51	14.43	10.78
8	PNZ	None	9.24	13.47	12.13
9	TPNZ-1	100°C/24h	16.94	16.55	16.36
10	TPNZ-2	225°C/3h	13.09	11.55	11.16
11	TPNZ-3	400°C/3h	15.40	14.63	14.05
12	CPNZ-1	NaCl	13.09	13.47	11.74
13	CPNZ-2	KCl	15.51	14.82	12.51
14	CPNZ-3	CaCl <sub>2</sub>	15.01	15.01	15.21
15	SNZ-1	None	22.33	21.56	20.59

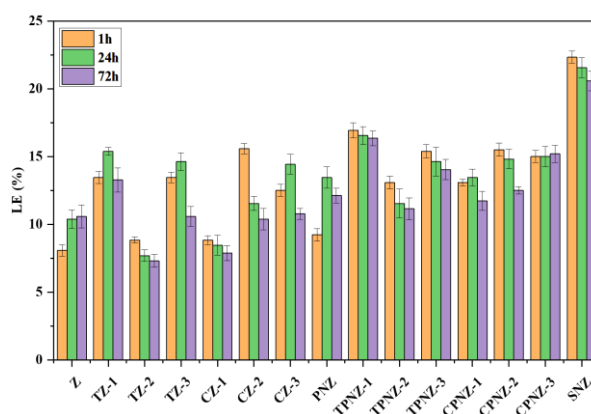


**Fig. 2** The LE% of Z, PNZ, modified Z, modified PNZ and SNZ after 3 different times (1h, 24h and 72h).

### 3.5. Dynamic laser scattering (DLS) measurements including hydrodynamic diameters and $\zeta$ -Potential (mV)

DLS measurements, including hydrodynamic diameter and zeta potential, were demonstrated in **Fig. 3a** and **3b**, respectively. The average particle size distribution of natural zeolite (Z) was recorded in 2 populations at peak II: 811.3 nm (81.0%) and peak I: 141.2 nm (19.0%). The average size distribution for TPNZ 1 and SNZ 1 was 87.6 nm and 233.8 nm, respectively. After adding urea, the average particle size increased in the 3 kinds of NPs, confirming that urea was successfully encapsulated. In U-CZ 2, the DLS size was observed in 2 populations at peak II 980.9 nm (82%) and I 153.6 nm (18%). Meanwhile, in U-TPNZ 1 and U-SNZ, the hydrodynamic diameter increased to around 111.3 nm and 360.0 nm, respectively. According to the poly dispersing index (PDI), which is an indication for uniformly prepared NPs, in particular, if its value is

less than 1.0, the results are as shown in **Fig. 3a**, the TPNZ 1 were more uniformly after U loading where this value was increased in U-CZ 2 compared to CZ-2. At the same time, there was no significant change in the PDI value for SNZ 1 and U-SNZ 1. According to  $\zeta$ -potential results, the negative charges of the samples were decreased from -11.9, 26.9 and 41.8 mV in CZ-2, TPNZ-1 and SNZ-1 to -8.6, 14.1 and -30.9 mV in U-CZ 2, U-TPNZ 1 and U-SNZ 1, respectively. Due to the higher amount of encapsulated urea in U-TPNZ 1 and U-SNZ 1, there was a higher decrease in their negative charges compared to U-Z.

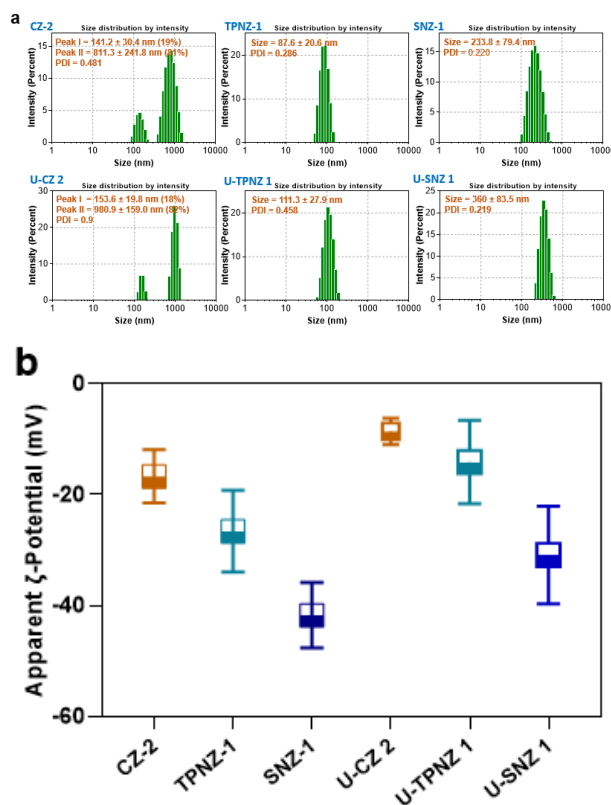


**Fig. 3** DLS hydrodynamic diameters of the produced CZ-2, TPNZ 1, SNZ 1 before and after urea (U) loading (A). Apparent  $\zeta$ -Potential (mV) CZ-2, TPNZ 1, SNZ 1 before and after U encapsulation (B)

### 3.6. TEM, SEM Imaging and EDX of NZ systems

The morphological characteristics of TPNZ 1 and SNZ 1 were examined using a scanning electron microscope (SEM), revealing that most of TPNZ 1 displayed spherical-shaped particles. At the same time, SNZ 1 showed cubic-shaped particles, as shown in **Fig. 4a** and **b**. This observation was further confirmed in TEM images. TPNZ 1 and SNZ 1 TEM images are presented in **Fig. 4c** and **d**, respectively. TPNZ 1 exhibited spherical-shaped particles in the nano-dimension, with a size ranging at the nano-scale diameter of  $14.3 \pm 4.2$  nm. The morphological surface of the physically prepared nanozeolite showed zeolite type X or Y (Si/Al=4.6) [98].

On the other hand, U-SNZ 1 displayed high homogeneity in the range of  $214.3 \pm 32.9$  nm. TEM examination confirmed the formation of the well-known cubic shape and structure of SNZ in a laboratory, with regular crystals of cubic shape obtained, indicating the successful formation of the characteristic lattice structure of the basic structural unit for type A zeolite. The difference between TEM and DLS measurements could be attributed to the fact that DLS measures dispersed particles in solutions, causing swelling of the measured particles, as interpreted in previous reports. The results of TEM examinations were consistent with reported findings [99][100].

EDX provided an in-situ study of zeolite's mineral and elemental composition, offering quantitative information on the Si/Al ratio. Si and Al are the main two elements in all tested samples. As depicted in **Fig. 5**, both Si and Al were recorded, indicating that all samples represent zeolite-based materials. According to **Fig. 5**, the Si/Al weight ratio estimated in CZ 2 and TPNZ 1 is 3.86 and 4.60, respectively. These results are consistent with previous studies, which reported that the Si/Al ratio falls within the range of 2 to 5 [101,102,103]. A small proportion of other cations, such as K<sup>+</sup>, Ca<sup>++</sup>, Mg<sup>++</sup>, and Na<sup>+</sup>, was also observed.

In the EDX analysis of SNZ 1, the total elemental composition of the sample revealed a significant content of Na<sup>+</sup>, which can be attributed to the use of NaOH during the preparation of SNZ 1. This indicates that the synthesized SNZ 1 was obtained with a high purity, contributing to its overall purity [67] [82]. Although Si was higher in SNZ 1, it appears lower in U-SNZ 1. This difference might be attributed to the fact that the loaded urea could have affected the detection of Si. EDX showed N peaks for the U-loaded samples, confirming that urea was successfully encapsulated. The N peak could be higher in U-TPNZ 1 and U-SNZ 1 than in U-CZ 2. It was observed that the N content was recorded at 4.3%, 15.4%, and 17.8% in U-CZ 2, U-TPNZ 1, and U-SNZ 1, respectively.

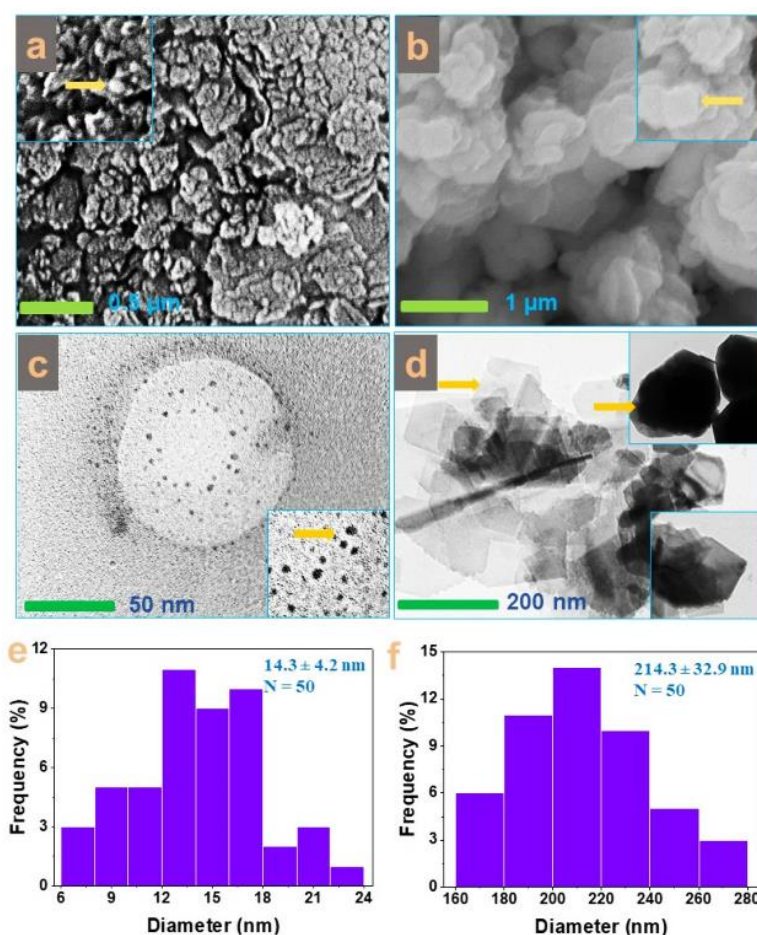


**Fig. 4.** SEM images of U-PNZ (a) and U-SNZ (b). TEM micrographs of U-PNZ (c) and U-SNZ (d). Histograms to declare the particle size distribution of U-PNZ (e) and U-SNZ (f), according to TEM images.

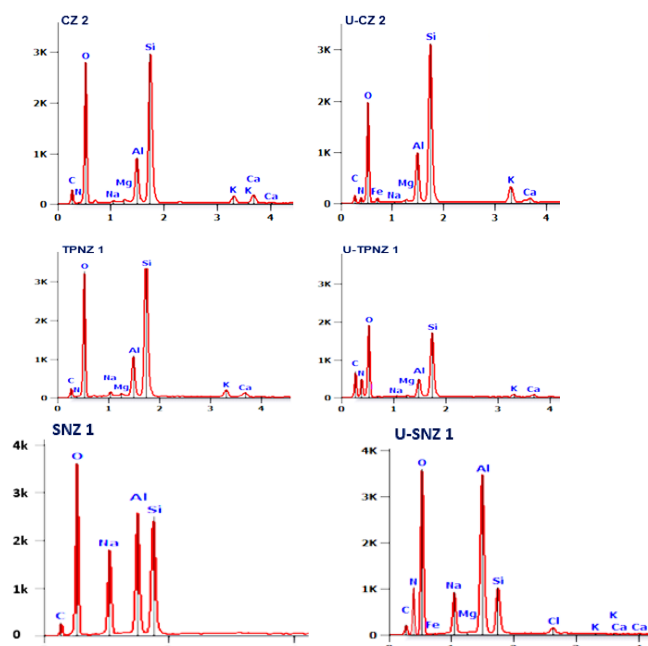


Fig. 5. EDX spectra of the CZ 2, TPNZ 1, SNZ 1 and their corresponding U-loaded forms

### 3.7. FTIR and RAMAN

The IR spectra of all samples were performed for urea U, CZ 2, TPNZ 1, SNZ 1 and their U-loaded forms to demonstrate the vibrations of the chemical bands at a wavelength in the range of 4000-100  $\text{cm}^{-1}$  as shown in **Fig. 6a**. Firstly, characteristic peaks of U powder were located at 3090-3600  $\text{cm}^{-1}$  due to the strong H-bonding which can be shared from surrounding OH-group of water molecules and from -NH<sub>2</sub> group of U and also can be shared from the OH-group of the internal structures of U sample [104]. The peak observed at 1155  $\text{cm}^{-1}$  corresponds to NH<sub>2</sub> stretching. The peak observed at 1463  $\text{cm}^{-1}$  could correspond to C-N stretching, which was noticed at 1686  $\text{cm}^{-1}$  due to C=O [104] [105].

For IR of CZ 2, the band located at 462  $\text{cm}^{-1}$  is attributed to the Si, Al-O band. The peaks observed at 608-794  $\text{cm}^{-1}$  are attributed to the symmetrical stretching vibration of Si-O-T (T = Si or Al), while the peak located at 1045  $\text{cm}^{-1}$  could correspond to the asymmetrical stretching vibration of Si-O-T. The 3100-3620  $\text{cm}^{-1}$  peaks correspond to Si-OH stretching and Si-OH bending vibration [106]. The characteristic bands of TPNZ1 appear to be similar to CZ 2. However, the strongest band was extended from 594-801  $\text{cm}^{-1}$ , representing the fingerprint linkage of TPNZ 1, which varies from CZ 2. There were changes in the locations and intensities of some peaks due to physical preparation and subsequent thermal treatment of TPNZ 1. For SNZ 1, the peak observed at 447  $\text{cm}^{-1}$  is attributed to internal vibrations of Si-O-Si and Si-O-Al bridges. The peaks observed at 1001 and 783  $\text{cm}^{-1}$  are attributed to asymmetric and symmetric stretches, respectively. Meanwhile, the bands observed at 3160-3600  $\text{cm}^{-1}$  originate from OH stretching and water absorbed by the zeolite.[107].

Ultimately, for U-loaded samples, it can be observed that most of their peaks were shifted and increased in intensity after loading with U. This change could be observed in the peaks located at 3100-3600  $\text{cm}^{-1}$ , particularly for U-TPNZ 1 and SNZ 1. Furthermore, it can be observed that peaks at 604 and 789  $\text{cm}^{-1}$  in TPNZ 1 and 447-783  $\text{cm}^{-1}$  in SNZ 1 mostly disappeared in their U-loaded forms, which indicated that the U was successfully encapsulated. This was also observed at 1045  $\text{cm}^{-1}$  in TPNZ 1 and 1001  $\text{cm}^{-1}$  in SNZ 1. However, this change was less in U-CZ 2. These observations indicated that U was more loaded in TPNZ 1 and SNZ 1 than CZ 2, consistent with the U-loading study.

The Raman spectra of all samples, CZ 2, TPNZ 1, SNZ 1 and their U-loaded forms were evaluated to record the behavior of the different samples' fingerprints, as shown in **Fig. 6b**. The characteristic peaks of zeolite-based materials can be detected in

the region of 300-970  $\text{cm}^{-1}$ . In SNZ 1, the characteristic peak at 476  $\text{cm}^{-1}$  is related to the strong bending of T-O symmetric stretch (T= Si/Al, O= oxygen). For CZ 2, this peak was observed at 473  $\text{cm}^{-1}$ , which could be attributed to the weak linkages from the T-O-T asymmetric stretch. Meanwhile, in TPNZ 1, the peak is 474  $\text{cm}^{-1}$  [8].

Also, it was noticed that the intensity of TPNZ 1 at 474  $\text{cm}^{-1}$  was decreased compared to CZ 2 as a result of producing more broken silica rings and broken edges during physical preparation and subsequent thermal treatment of TPNZ 1. This peak was of higher intensity in SNZ 1. For U-loaded samples, it was observed that the intensities were changed with slight shifts, which could be attributed to this strong bonding between the internal structure of samples and nitrogen in U. Thus, it was observed that the dominant effect of the strong H-bonding of samples and in U-CZ 2 in reducing the intensity at 475  $\text{cm}^{-1}$ , while the peak observed at 595 shifted to 679  $\text{cm}^{-1}$  in U-CZ 2. Also, the peaks observed at 1453 and 1517  $\text{cm}^{-1}$  in SNZ 1 can be related to stretching bands such as C-N and C=O. This was observed at 1456 and 1516  $\text{cm}^{-1}$  in CZ 2 and at 1456 and 1519  $\text{cm}^{-1}$  in TPNZ 1. The intensities of these peaks and positions were changed after loading with U. Furthermore, it can be observed that some peaks appeared as a result of loading U, where these peaks can be related to the water molecules or bonding between the amino group of U and oxygen of samples, and can be related to the OH-bonding between the internal structure of samples or water molecules and the amino group of urea. Therefore, from the Raman shift, the diffusion of urea into samples by strong bonding led to a change in peak intensities and positions, with the appearance of new peaks. From Raman spectra and IR spectra, it could be concluded that U was successfully encapsulated.

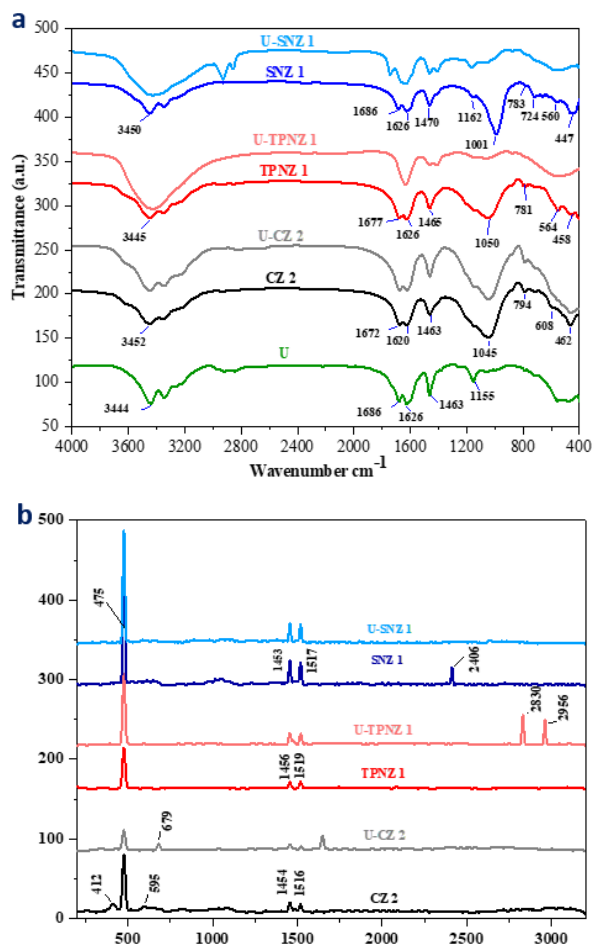


**Fig. 6.** FTIR spectra (a) and NMR spectra (b) for CZ-2, TPNZ 1, SNZ 1 and their U-loaded forms.

### 3.8. Surface area and Pore properties

The samples' surface area and pore properties were assessed through isotherm models of nitrogen gas adsorption and desorption at 196°C [108][109]. This analysis employed the Brunauer-Emmett-Teller (BET) surface area analysis method. BET involves a multi-point measurement of the specific surface area (m<sup>2</sup>/g) through gas adsorption analysis. In this process, an inert gas like nitrogen (N<sub>2</sub>) is continuously passed over the solid sample or the solid sample is suspended in a defined gaseous volume.

As shown in **Fig. 7**, the amount adsorbed of N<sub>2</sub> gas related to the entire surface area was assessed and expressed in samples by units of area per gas' mass (cc/g). It was recorded at 251.07, 205.23 and 130.60 cc/g, in SNZ 1, TPNZ 1 and CZ 2, respectively.

The specific surface area and pore size distribution data were analyzed using the BET Microsoft analysis system, and the results are presented in **Table 4**. The specific surface areas of CZ 2, TPNZ 1, and SNZ 1 were determined to be 254.22, 399.49, and 487.01 m<sup>2</sup>/g, respectively. The maximum volume of pores was observed in SNZ 1. The average pore size for CZ 2, TPNZ 1, and SNZ 1 was measured at 11.59, 1.59, and 1.60 nm, respectively. The total pore volume was also recorded as 0.2, 0.32, and 0.4 cc/g for CZ 2, TPNZ 1, and SNZ 1, respectively. These results indicate that TPNZ 1 and SNZ 1 possess higher specific surface areas and pore volumes than CZ 2, emphasizing their potential as effective adsorbents for urea molecules.

The results from BET analysis, encompassing surface area, pore volume, and pore size distribution for the tested samples, affirm previous findings that urea (U) was loaded more effectively in TPNZ 1 and SNZ 1 compared to CZ 2. This can be attributed to the higher surface area and increased porosity of both NZ systems (TPNZ 1 and SNZ 1), facilitating the incorporation of urea molecules into their structure. Moreover, this highlights the influence of nano-dimension on augmenting the surface area in zeolite, acting as an adsorbent material for urea fertilizer, and enhancing nitrogen-urea loading efficiency.

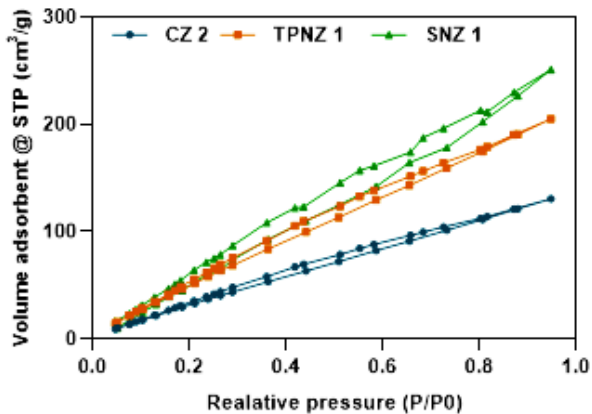


**Fig. 7.** Isotherm curves for the amount adsorbed of N<sub>2</sub> (cc/g) per relative pressure (P/P<sub>0</sub>) of samples CZ 2, TPNZ 1 and SNZ 1.

**Table 4.** The surface area and pore properties of CZ 2, TPNZ 1 and SNZ 1

Properties	Z	PNZ	SNZ 1
Surface Area			
m <sup>2</sup> /g	254.22	399.49	487.01
Average Pore			
Size nm	1.59	1.59	1.60
Total Pore			
Volume cc/g	0.20	0.32	0.40

### 3.9. In-vitro release studies

After quantifying the total nitrogen content loaded on the zeolite, the nitrogen release study was carried out in two release media, water and soil columns, as previously described. The release study involved commercial urea, U-CZ 1, U-TPNZ 1, and U-SNZ 1. In the release patterns of urea in water, as depicted in **Fig. 8a**, it was observed that free urea was primarily released within the first 6 hours. U-CZ 2 exhibited the release of over 91% of the loaded urea in the initial two days, followed by a slow release until the end of the study. After two days, U-SNZ 1 released approximately 84% of the loaded urea, while U-TPNZ 1 released a lesser amount, around 70%. U-TPNZ 1 and U-SNZ 1 released urea gradually and sustainably after two days. By the conclusion of the release study (after 480 hours), approximately 93%, 85%, and 81% of the encapsulated urea were released in U-CZ 1, U-SNZ 1, and U-TPNZ 1, respectively.

U-PNZ demonstrates efficacy as a carrier for delivering urea slowly and sustainably over an extended period.

The release study was also documented in soil columns, as depicted in **Fig. 8b**. It was observed that 100% of the commercial urea was released on the third day. After five days, U-CZ 2 released approximately 80% of the loaded urea, gradually reaching 94% by day 12 and 96% by day 20. In contrast, SNZ 1 exhibited a slower release pattern, with around 74% of the loaded urea released on the fifth day. The slowest release pattern was observed in TPNZ 1, removing 62% of urea after 5 days. Subsequently, the urea release continued gradually in both NZ systems, U-SNZ 1 and U-TPNZ 1, reaching 84% and 76% of the loaded urea, respectively, by the end of the 20-day study period. No significant difference in releasing efficiency was noted among the tested samples in both water and sand. Both NZ systems, U-SNZ 1 and U-TPNZ 1, demonstrated greater efficiency as promising nanocarriers for releasing urea, mainly when tested in soil. However, TPNZ 1 exhibited a slower and more sustained release than SNZ 1, possibly due to the larger nanopores in SNZ 1, allowing for easier detachment and faster release of adsorbed urea molecules in water or sandy soil compared to TPNZ 1.

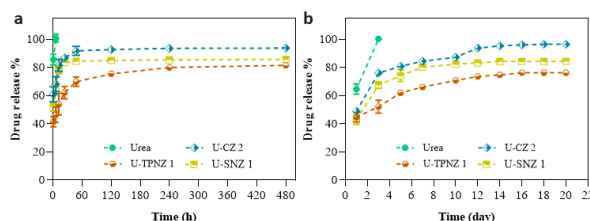


**Fig. 8.** Cumulative release percentages of U from U-CZ 2, U-TPNZ 1 and U-SNZ 1 in water (a) and in soil (b)

### 3.10. The productivity of the U-loaded NZs of lettuce growth

In a pot experiment designed to assess the impact of utilizing NZ systems as a nutrient source on the growth of lettuce (a vegetable plant), various growth parameters were measured, including plant length, number of leaves, fresh weight, and total nitrogen and protein contents in leaves, as shown in **Fig. 9**. The results indicated an increase in plant growth parameters, mainly when grown with the recommended dose of urea. Notably, plants grown in the presence of U-SNZ 1 and U-TPNZ 1 exhibited greater fresh weight than those treated with commercial urea and U-CZ 2 when utilizing the recommended dose of urea. U-TPNZ 1 and U-SNZ 1 displayed 2.7- and 2.9-fold increases compared to control samples in fresh weight. Moreover, nitrogen and protein contents were enhanced when using U-TPNZ 1 and U-SNZ 1. Both NZ systems increased nitrogen and protein contents from 0.58% and 10.0% in the control to 1.3% and 22.5% in U-TPNZ 1 and 1.5% and 26.1%, respectively. This improvement in protein and nitrogen contents was also observed when utilizing 50% of the recommended sample dosage. There was also an increase in protein and nitrogen using U-CZ 2, although to a lesser extent; however, it remained higher than commercial urea at 50% or 100% of the recommended dosage.

Furthermore, when utilizing 100% of the recommended dosage, the number of leaves, leaf length, and root length increased when using U-TPNZ 1 and U-SNZ 1, compared to the control, commercial urea (U), and U-CZ 2.

The results indicated that both NZs, specifically U-TPNZ 1 and U-SNZ 1, demonstrated the most effective treatment as nano-dimension zeolites. This is likely due to their enhanced capacity to retain nutrients and water in the root zone more efficiently than micro-dimension zeolite or commercial urea. The sustained release pattern of nitrogen observed in the in-vitro release studies likely contributes to this improved efficiency. The study highlighted that TPNZ 1, produced from treated natural Z, efficiently adsorbs urea molecules and releases them slowly in a sustained manner, potentially enhancing the growth rates of vegetable plants compared to commercial urea or U-CZ 2. Additionally, U-TPNZ 1 exhibited a slow urea release similar to U-SNZ 1, and their effects on lettuce growth and growth parameters were comparable. Consequently, TPNZ 1 could be considered a promising platform for further studies to optimize its use as nanocarriers for urea, potentially offering better growth rate efficiency than U-SNZ 1.

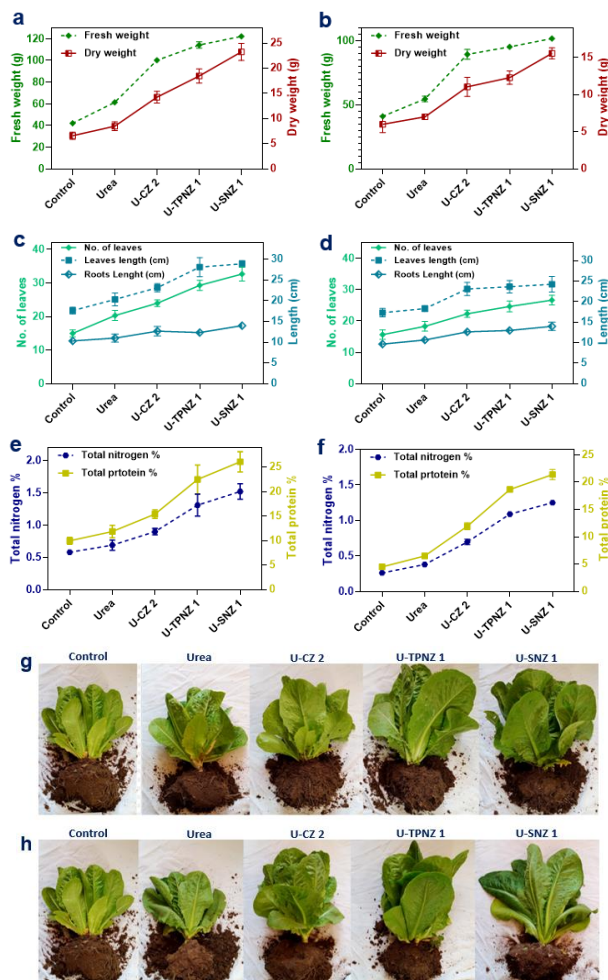


**Fig. 9.** Effect of utilizing NZ systems at 100% of the recommended dosage, on the growth scale of lettuce through measuring fresh an and dry weight (a), number of leaves, root and leave length (c) and total nitrogen and protein contents (e). Effect of utilizing NZ systems at 50% of the recommended dosage, on the growth scale of lettuce through measuring fresh an and dry weight (b), number of leaves, root and leave length (d) and total nitrogen and protein contents (f). Image of lettuce grown in the presence of sample at 100% (g) and 50% (h) of the recommended dosage.

### Conclusion

In summary, the study utilized different approaches to develop natural zeolite and produce PNZ as environmentally friendly materials and promising nanocarriers for urea in the field of agriculture. Such approach will overcome the commercial urea fertilizer associated drawbacks, through reducing nitrogen losses in soil, and water, and the environmental hazards. The

optimization of specific sites on the urea surfaces was achieved to enhance the urea loading capacity, thereby improving the efficiency of nitrogen content. Thermal and chemical modifications were employed for this purpose. The study employed simple and applicable methods for preparing NZ in the laboratory, using eco-friendly and biodegradable materials, such as agricultural wastes or recycled materials, on a small or large scale. Characterization techniques such as DLS, XRD, FTIR, SEM-EDX, and TEM were utilized to characterize the nanoparticles (NPs) produced. Encapsulation capacity and release studies were conducted. The findings revealed that the treated natural Z had TPNZ 1 efficiently adsorbed urea molecules and released them slowly and sustainably. This property could potentially enhance vegetable plants' growth rates compared to commercial urea or U-CZ 2. The developed TPNZ 1 could be considered a promising platform for further studies to refine its use as nanocarriers for urea, potentially offering better growth rate efficiency than SNZ 1.

### Conflict of Interest

The authors declare that they have no relevant affiliations or financial involvement with any organization or entity that has a financial interest in or conflict with the subject matter or materials discussed in the manuscript. This includes employment, consultancies, honoraria, stock ownership or options, expert testimony, grants or patents received or pending, or royalties.

### References

- [1] World fertilizer trends and outlook to 2022, World Fertil. Trends Outlook to 2022. (2020). <https://doi.org/10.4060/ca6746en>.
- [2] X. Jin, G. Yang, C. Tan, C. Zhao, Effects of nitrogen stress on the photosynthetic CO<sub>2</sub> assimilation, chlorophyll fluorescence, and sugar-nitrogen ratio in corn, *Sci. Rep.* 5 (2015). <https://doi.org/10.1038/SREP09311>.
- [3] I. Pikaar, S. Matassa, K. Rabaey, B.L. Bodirsky, A. Popp, M. Herrero, W. Verstraete, *Microbes and the Next Nitrogen Revolution*, (2017). <https://doi.org/10.1021/acs.est.7b00916>.
- [4] R. Gil-Ortiz, M.Á. Naranjo, A. Ruiz-Navarro, M. Caballero-Molada, S. Atares, C. García, O. Vicente, *New Eco-Friendly Polymeric-Coated Urea Fertilizers Enhanced Crop Yield in Wheat*, (n.d.), (2020). <https://doi.org/10.3390/agronomy10030438>.
- [5] M.Y. Naz, S.A. Sulaiman, Slow release coating remedy for nitrogen loss from conventional urea: a review, *J. Control. Release.* 225 (2016) 109–120. <https://doi.org/10.1016/J.JCONREL.2016.01.037>.
- [6] A.J. Messiga, K. Dyck, K. Ronda, K. Van Baar, D. Haak, S. Yu, M. Dorais, *Nutrients Leaching in Response to Long-Term Fertigation and Broadcast Nitrogen in Blueberry Production*, (2020). <https://doi.org/10.3390/plants9111530>.
- [7] Y. Jia, Z. Hu, Y. Ba, W. Qi, Application of biochar-coated urea controlled loss of fertilizer nitrogen and increased nitrogen use efficiency, *Chem. Biol. Technol. Agric.* 8 (2021) 1–11. <https://doi.org/10.1186/s40538-020-00205-4>.
- [8] Y. Zhang, X. Liang, X. Yang, H. Liu, J. Yao, *An Eco-Friendly Slow-Release Urea Fertilizer Based on Waste Mulberry Branches for Potential Agriculture and Horticulture Applications*, *ACS Sustain. Chem. Eng.* 2 (2014) 1871–1878. <https://doi.org/10.1021/sc500204z>.
- [9] A.J. Messiga, X. Hao, M. Dorais, C.S. Bineng, N. Ziadi, A. Messiga, C. Bineng, X. Hao, M. Dorais, N. Ziadi, *ARTICLE Supplement of biochar and vermicompost amendments in coir and peat growing media improves N management and yields of leafy vegetables 1*, *Can. J. Soil Sci.* 102 (n.d.), (2020) 39–52. <https://doi.org/10.1139/cjss-2020-0059>.
- [10] M.A. Aslam, I. Aziz, S.H. Shah, S. Muhammad, M. Latif, A. Khalid, *Effects of Biochar and Zeolite Integrated With Nitrogen on Soil Characteristics, Yield and Quality of Maize (Zea Mays L.)*, *Pakistan J. Bot.* 53 (2021) 2047–2057. [https://doi.org/10.30848/PJB2021-6\(27\)](https://doi.org/10.30848/PJB2021-6(27)).
- [11] D. Lawrenciana, S.K. Wong, D. Yi, S. Low, H. Goh, J.K. Goh, U.R. Ruktanonchai, A. Soottitawat, H. Lee, S.Y. Tang, D.; Lawrenciana, S.K.; Wong, D.Y.S.; Low, B.H.; Goh, J.K.; Goh, *plants Controlled Release Fertilizers: A Review on Coating Materials and Mechanism of Release*, (2021). <https://doi.org/10.3390/plants10020238>.
- [12] C. Janke, P. Moody, R. Fujinuma, M. Bell, *The Impact of Banding Polymer-Coated Urea on Nitrogen Availability and Distribution in Contrasting Soils*, *J. Soil Sci. Plant Nutr.* 22 (2022) 3081–3095. <https://doi.org/10.1007/s42729-022-00869-x>.
- [13] E.G. Arafa, M.W. Sabaa, R.R. Mohamed, E.M. Kamel, A.M. Elzanaty, A.M. Mahmoud, O.F. Abdel-Gawad, *Eco-friendly and biodegradable sodium alginate/quaternized chitosan hydrogel for controlled release of urea and its antimicrobial activity*, *Carbohydr. Polym.* 291 (2022) 119555. <https://doi.org/10.1016/J.CARBPOL.2022.119555>.
- [14] K. Saurabh, M. Kanchikeri Math, S.C. Datta, A.S. Thekkumpurath, R. Kumar, *Nanoclay polymer composites loaded with urea and nitrification inhibitors for controlling nitrification in soil*, *Arch. Agron. Soil Sci.* 65 (2019) 478–491. <https://doi.org/10.1080/03650340.2018.1507023>.
- [15] P. Goswami, J. Mathur, N. Srivastava, *Silica nanoparticles as novel sustainable approach for plant growth and crop protection*, (2022). <https://doi.org/10.1016/j.heliyon.2022.e09908>.
- [16] C. Tarafder, M. Daizy, M. Morshed Alam, M. Ripon Ali, M. Jahidul Islam, R. Islam, M. Sohel Ahommed, M. Aly Saad Aly, M. Zaved Hossain Khan, *Formulation of a Hybrid Nanofertilizer for Slow and Sustainable Release of*

- Micronutrients, (2020). <https://doi.org/10.1021/acsomega.0c03233>.
- [17] O.M. Elshayb, A.M. Nada, K.Y. Farroh, A.A. AL-Huqail, M. Aljabri, N. Binothman, M.F. Seleiman, Utilizing Urea–Chitosan Nanohybrid for Minimizing Synthetic Urea Application and Maximizing *Oryza sativa* L. Productivity and N Uptake, *Agriculture*. 12 (2022) 944. <https://doi.org/10.3390/agriculture12070944>.
- [18] S. Zhang, X. Fu, Z. Tong, G. Liu, S. Meng, Y. Yang, M.I.D. Helal, Y.C. Li, Lignin-Clay Nanohybrid Biocomposite-Based Double-Layer Coating Materials for Controllable-Release Fertilizer, *ACS Sustain. Chem. Eng.* 8 (2020) 18957–18965. <https://doi.org/10.1021/acssuschemeng.0c06472>.
- [19] M.I.D. Helal, Z. Tong, H.A. Khater, M.A. Fathy, F.E. Ibrahim, Y. Li, N.H. Abdelkader, Modification of Fabrication Process for Prolonged Nitrogen Release of Lignin–Montmorillonite Biocomposite Encapsulated Urea, *Nanomaterials*. 13 (2023) 1889. <https://doi.org/10.3390/nano13121889>.
- [20] M.I.D. Helal, M.M. El-Mogy, H.A. Khater, M.A. Fathy, F.E. Ibrahim, Y.C. Li, Z. Tong, K.F. Abdelgawad, A Controlled-Release Nanofertilizer Improves Tomato Growth and Minimizes Nitrogen Consumption, *Plants*. 12 (2023) 1978. <https://doi.org/10.3390/PLANTS12101978/S1>.
- [21] R. Chakraborty, A. Mukhopadhyay, S. Paul, S. Sarkar, R. Mukhopadhyay, Nanocomposite-based smart fertilizers: A boon to agricultural and environmental sustainability, *Sci. Total Environ.* 863 (2023) 160859. <https://doi.org/10.1016/J.SCITOTENV.2022.160859>.
- [22] N. Sobuś, I. Czekaj, V. Diichuk, I.M. Kobasa, Characteristics of the structure of natural zeolites and their potential application in catalysis and adsorption processes, *Tech. Trans.* (2020) 1–20. <https://doi.org/10.37705/TechTrans/e2020043>.
- [23] C. Colella, W.S. Wise, The IZA Handbook of Natural Zeolites: A tool of knowledge on the most important family of porous minerals, *Microporous Mesoporous Mater.* 189 (2014) 4–10. <https://doi.org/10.1016/J.MICROMESO.2013.08.028>.
- [24] R. Vajtai, ed., *Springer Handbook of Nanomaterials*, Springer Berlin Heidelberg, Berlin, Heidelberg, 2013. <https://doi.org/10.1007/978-3-642-20595-8>.
- [25] M. Moshoeshoe, M. Silas Nadiye-Tabbiruka, V. Obuseng, A Review of the Chemistry, Structure, Properties and Applications of Zeolites, *Am. J. Mater. Sci.* 2017 (2017) 196–221. <https://doi.org/10.5923/j.materials.20170705.12>.
- [26] N.R. Mijailović, B. Nedić Vasiljević, M. Ranković, V. Milanović, S. Uskoković-Marković, Environmental and Pharmacokinetic Aspects of Zeolite/Pharmaceuticals Systems—Two Facets of Adsorption Ability, *Catalysts*. 12 (2022) 837. <https://doi.org/10.3390/catal12080837>.
- [27] K. Stocker, M. Ellersdorfer, M. Lehner, J.G. Raith, Characterization and Utilization of Natural Zeolites in Technical Applications, *BHM Berg- Und Hüttenmännische Monatshefte*. 162 (2017) 142–147. <https://doi.org/10.1007/s00501-017-0596-5>.
- [28] A.T. Ahmed, H. Almohamadi, Chemical and microstructural studies for using natural zeolite in advanced wastewater treatment, *Int. J. Environ. Sci. Technol.* 20 (2023) 6491–6498. <https://doi.org/10.1007/s13762-022-04384-5>.
- [29] K. Narang, F. Akhtar, molecules Freeze Granulated Zeolites X and A for Biogas Upgrading, (n.d.) (2020). <https://doi.org/10.3390/molecules25061378>.
- [30] E. Pérez-Botella, S. Valencia, F. Rey, Zeolites in Adsorption Processes: State of the Art and Future Prospects, (2022). <https://doi.org/10.1021/acs.chemrev.2c00140>.
- [31] T. Ennaert, V. Aelst, J. Dijkmans, R. De Clercq, W. Schutyser, M. Dusselier, D. Verboekend, B.F. Sels, Potential and challenges of zeolite chemistry in the catalytic conversion of biomass, *Chem. Soc. Rev.* 584 (2016) 584. <https://doi.org/10.1039/c5cs00859j>.
- [32] Concepts of modern technologies of obtaining valuable biomass-derived chemicals, *Czas. Tech.* 8 (2018). <https://doi.org/10.4467/2353737XCT.18.114.8889>.
- [33] T.P. Prasai, K.B. Walsh, S.P. Bhattarai, D.J. Midmore, T.T.H. Van, R.J. Moore, D. Stanley, Zeolite food supplementation reduces abundance of enterobacteria, *Microbiol. Res.* 195 (2017) 24–30. <https://doi.org/10.1016/J.MICRES.2016.11.006>.
- [34] C.C. Villa, G.A. Valencia, A. López Córdoba, R. Ortega-Toro, S. Ahmed, T.J. Gutiérrez, Zeolites for food applications: A review, *Food Biosci.* 46 (2022) 101577. <https://doi.org/10.1016/J.FBIO.2022.101577>.
- [35] P. Sharma, P.P. Sutar, H. Xiao, Q. Zhang, The untapped potential of zeolites in techno-augmentation of the biomaterials and food industrial processing operations: a review, *J. Futur. Foods*. 3 (2023) 127–141. <https://doi.org/10.1016/J.JFUTFO.2022.12.004>.
- [36] N. Eroglu, M. Emekci, C.G. Athanassiou, Applications of natural zeolites on agriculture and food production, (2017). <https://doi.org/10.1002/jsfa.8312>.
- [37] E. Cataldo, L. Salvi, F. Paoli, M. Fucile, G. Masciandaro, D. Manzi, C.M. Masini, G.B. Mattii, Application of Zeolites in Agriculture and Other Potential Uses: A Review, *Agronomy*. 11 (2021) 1547. <https://doi.org/10.3390/agronomy11081547>.
- [38] M. Mondal, B. Biswas, S. Garai, S. Sarkar, H. Banerjee, K. Brahmachari, P.K. Bandyopadhyay, S. Maitra, M. Brestic, M. Skalicky, P. Ondrisik, A. Hossain, Zeolites Enhance Soil Health, Crop Productivity and Environmental Safety, *Agronomy*. 11 (2021) 448. <https://doi.org/10.3390/agronomy11030448>.
- [39] S.A.A. Nakhli, M. Delkash, B.E. Bakhshayesh, H. Kazemian, Application of Zeolites for Sustainable Agriculture: a Review on Water and Nutrient Retention, *Water, Air, Soil Pollut.* 228 (2017) 464. <https://doi.org/10.1007/s11270-017-3649-1>.
- [40] M. Ayari, A. Charef, R. Azouzi, N. Khiari, M. Ben Sassi, Effect of Zeolite, Femur and Lignite Application Rates on Soil Hydraulic Properties and Fertility of Sandy and Clay Soils at Semi-arid Climate, *Commun. Soil Sci. Plant Anal.*

- 53 (2022) 408–425. <https://doi.org/10.1080/00103624.2021.2017446>.
- [41] K. Ramesh, D.D. Reddy, Chapter Four - Zeolites and Their Potential Uses in Agriculture, in: D.L.B.T.-A. in A. Sparks (Ed.), *Adv. Agron.*, Academic Press, 2011: pp. 219–241. <https://doi.org/https://doi.org/10.1016/B978-0-12-386473-4.00004-X>.
- [42] P.J. Leggo, An investigation of plant growth in an organo-zeolitic substrate and its ecological significance, *Plant Soil*. 219 (2000) 135–146. <https://doi.org/10.1023/A:1004744612234>.
- [43] U. Geological Survey, MINERAL COMMODITY SUMMARIES 2021, (n.d.).
- [44] K. Margeta, N. Zabukovec Logar, M. Šiljeg, A. Farkaš, Natural Zeolites in Water Treatment-How Effective is Their Use, (2013). <https://doi.org/10.5772/50738>.
- [45] A. Khaleque, M.M. Alam, M. Hoque, S. Mondal, J. Bin Haider, B. Xu, M.A.H. Johir, A.K. Karmakar, J.L. Zhou, M.B. Ahmed, M.A. Moni, Zeolite synthesis from low-cost materials and environmental applications: A review, *Environ. Adv.* 2 (2020) 100019. <https://doi.org/10.1016/J.ENVADV.2020.100019>.
- [46] W. He, H. Gong, K. Fang, F. Peng, K. Wang, Revealing the effect of preparation parameters on zeolite adsorption performance for low and medium concentrations of ammonium, *J. Environ. Sci.* 85 (2019) 177–188. <https://doi.org/10.1016/J.JES.2019.05.021>.
- [47] B. Kozera-Sucharda, B. Gworek, I. Kondzielski, The Simultaneous Removal of Zinc and Cadmium from Multicomponent Aqueous Solutions by Their Sorption onto Selected Natural and Synthetic Zeolites, *Minerals*. 10 (2020) 343. <https://doi.org/10.3390/min10040343>.
- [48] M.F. Mubarak, A.M.G. Mohamed, M. Keshawy, T.A. elMoghny, N. Shehata, Adsorption of heavy metals and hardness ions from groundwater onto modified zeolite: Batch and column studies, *Alexandria Eng. J.* 61 (2022) 4189–4207. <https://doi.org/10.1016/j.aej.2021.09.041>.
- [49] A. Dziedzicka, B. Sulikowski, M. Ruggiero-Mikołajczyk, Catalytic and physicochemical properties of modified natural clinoptilolite, *Catal. Today*. 259 (2016) 50–58. <https://doi.org/10.1016/J.CATTOD.2015.04.039>.
- [50] N. Lihareva, · O Petrov, · L Dimowa, · Y Tzvetanova, · I Piroeva, · F Ublekov, · A Nikolov, Ion exchange of Cs + and Sr 2+ by natural clinoptilolite from bi-cationic solutions and XRD control of their structural positioning, *J. Radioanal. Nucl. Chem.* 323 (2020) 1093–1102. <https://doi.org/10.1007/s10967-020-07018-7>.
- [51] Z. Znak, O. Zin, A. Mashtaler, S. Korniy, Y. Sukhatskiy, P.R. Gogate, R. Mnykh, P. Thanekar, Improved modification of clinoptilolite with silver using ultrasonic radiation, *Ultrason. Sonochem.* 73 (2021) 105496. <https://doi.org/10.1016/J.ULTSONCH.2021.105496>.
- [52] E.C.G. Dignos, K.E.A. Gabejan, E.M. Olegario-Sanchez, H.D. Mendoza, The comparison of the alkali-treated and acid-treated naturally mined Philippine zeolite for adsorption of heavy metals in highly polluted waters, *IOP Conf. Ser. Mater. Sci. Eng.* 478 (2019) 012030. <https://doi.org/10.1088/1757-899X/478/1/012030>.
- [53] J. Cieśła, W. Franus, M. Franus, K. Kedziora, J. Gluszczyk, J. Szerement, G. Jozefaciuk, Environmental-Friendly Modifications of Zeolite to Increase Its Sorption and Anion Exchange Properties, *Physicochemical Studies of the Modified Materials, Materials (Basel)*. 12 (2019) 3213. <https://doi.org/10.3390/ma12193213>.
- [54] V. Yadav, M. Rani, L. Kumar, N. Singh, V. Ezhilselvi, Effect of Surface Modification of Natural Zeolite on Ammonium Ion Removal from Water Using Batch Study: an Overview, *Water, Air, Soil Pollut.* 233 (2022) 465. <https://doi.org/10.1007/s11270-022-05948-4>.
- [55] J. Shi, Z. Yang, H. Dai, X. Lu, L. Peng, X. Tan, L. Shi, R. Fahim, Preparation and application of modified zeolites as adsorbents in wastewater treatment, *Water Sci. Technol.* 2017 (2018) 621–635. <https://doi.org/10.2166/wst.2018.249>.
- [56] G. hua Liu, Y. Wang, Y. Zhang, X. Xu, L. Qi, H. Wang, Modification of natural zeolite and its application to advanced recovery of organic matter from an ultra-short-SRT activated sludge process effluent, *Sci. Total Environ.* 652 (2019) 1366–1374. <https://doi.org/10.1016/J.SCITOTENV.2018.10.334>.
- [57] F. Ogata, N. Nagai, C. Ito, Y. Kobayashi, M. Yamaguchi, A. Tabuchi, C. Saenjum, T. Nakamura, N. Kawasaki, Improvement in adsorption of Hg2+ from aqueous media using sodium-type fine zeolite grains, *Water Sci. Technol.* 85 (2022) 2827–2839. <https://doi.org/10.2166/wst.2022.126>.
- [58] V.J. Inglezakis, A. Kudarova, A. Guney, N. Kinayat, Z. Tauanov, Efficient mercury removal from water by using modified natural zeolites and comparison to commercial adsorbents, *Sustain. Chem. Pharm.* 32 (2023) 101017. <https://doi.org/10.1016/J.SCP.2023.101017>.
- [59] W. Lu, C. Zhang, P. Su, X. Wang, W. Shen, B. Quan, Z. Shen, L. Song, Research progress of modified natural zeolites for removal of typical anions in water, *Environ. Sci. Water Res. Technol.* 8 (2022) 2170–2189. <https://doi.org/10.1039/D2EW00478J>.
- [60] V. Sharma, B. Javed, H. Byrne, J. Curtin, F. Tian, Zeolites as Carriers of Nano-Fertilizers: From Structures and Principles to Prospects and Challenges, *Appl. Nano.* 3 (2022) 163–186. <https://doi.org/10.3390/applnano3030013>.
- [61] E. Wibowo, M. Rokhmat, Sutisna, R. Murniati, Khairurrijal, M. Abdullah, Thermally Activated Clay to Compete Zeolite for Seawater Desalination, *Adv. Mater. Res.* 1112 (2015) 154–157. <https://doi.org/10.4028/www.scientific.net/amr.1112.154>.
- [62] E. Wibowo, Sutisna, M. Rokhmat, R. Murniati, Khairurrijal, M. Abdullah, Utilization of Natural Zeolite as Sorbent Material for Seawater Desalination, in: *Procedia Eng.*, Elsevier Ltd, 2017: pp. 8–13. <https://doi.org/10.1016/j.proeng.2017.03.002>.
- [63] L. Lin, Z. Lei, L. Wang, X. Liu, Y. Zhang, C. Wan, D.J. Lee, J.H. Tay, Adsorption mechanisms of high-levels of ammonium onto natural and NaCl-modified zeolites, *Sep. Purif. Technol.* 103 (2013) 15–20. <https://doi.org/10.1016/j.seppur.2012.10.005>.

- [64] K. Ham, B.S. Kim, K.Y. Choi, Enhanced ammonium removal efficiency by ion exchange process of synthetic zeolite after Na<sup>+</sup> and heat pretreatment, *Water Sci. Technol.* 78 (2018) 1417–1425. <https://doi.org/10.2166/wst.2018.420>.
- [65] Thiquynhxuan Le, T. Wang, A. V. Ravindra, Y. Xuxiang, S. Ju, L. Zhang, Fast Synthesis of Submicron Zeolite Y Using Microwave Heating, *Kinet. Catal.* 62 (2021) 436–444. <https://doi.org/10.1134/S0023158421030046>.
- [66] Y. Li, H. Chen, J. Liu, W. Yang, Microwave synthesis of LTA zeolite membranes without seeding, *J. Memb. Sci.* 277 (2006) 230–239. <https://doi.org/10.1016/j.memsci.2005.10.033>.
- [67] M.M. Selim, D.M. EL-Mekkawi, R.M.M. Aboelenin, S.A. Sayed Ahmed, G.M. Mohamed, Preparation and characterization of Na-A zeolite from aluminum scrub and commercial sodium silicate for the removal of Cd<sup>2+</sup> from water, *J. Assoc. Arab Univ. Basic Appl. Sci.* 24 (2017) 19–25. <https://doi.org/10.1016/j.jaubas.2017.05.002>.
- [68] A. Khaleque, M.M. Alam, M. Hoque, S. Mondal, J. Bin Haider, B. Xu, M.A.H. Johir, A.K. Karmakar, J.L. Zhou, M.B. Ahmed, M.A. Moni, Zeolite synthesis from low-cost materials and environmental applications: A review, *Environ. Adv.* 2 (2020). <https://doi.org/10.1016/j.envadv.2020.100019>.
- [69] S. Proding, M.A. Derewinski, Synthetic zeolites and their characterization, INC, 2020. <https://doi.org/10.1016/b978-0-12-818487-5.00003-0>.
- [70] M.Z. Htun, M.M.H., Htay, M.M. and Lwin, Preparation of Zeolite (NaX, Faujasite) from Pure Silica and Alumina Sources, *Int. Conf. Chem. Process. Environ. Issues (ICCEEI)*, Singapore. (2012) 212–216.
- [71] S.N. Azizi, M. Yousefpour, Synthesis of zeolites NaA and analcime using rice husk ash as silica source without using organic template, *J. Mater. Sci.* 45 (2010) 5692–5697. <https://doi.org/10.1007/s10853-010-4637-7>.
- [72] S. Krachumram, K.C. Chanapatharapol, N. Kamonsuthipajit, Synthesis and characterization of NaX-type zeolites prepared by different silica and alumina sources and their CO<sub>2</sub> adsorption properties, *Microporous Mesoporous Mater.* 310 (2021) 110632. <https://doi.org/10.1016/j.micromeso.2020.110632>.
- [73] A. María Alvarez, D. Bola~ Nos Guerr, C. Montero Calder On, Natural zeolite as a chromium VI removal agent in tannery effluents, (2021). <https://doi.org/10.1016/j.heliyon.2021.e07974>.
- [74] George Estefan, *Methods of Soil, Plant, and Water Analysis: A manual for the West Asia and North Africa Region: Third Edition*, 3rd ed., 2013.
- [75] M.Z.H. Khan, M.R. Islam, N. Nahar, M.R. Al-Mamun, M.A.S. Khan, M.A. Matin, Synthesis and characterization of nanozeolite based composite fertilizer for sustainable release and use efficiency of nutrients, *Heliyon.* 7 (2021) e06091. <https://doi.org/10.1016/j.heliyon.2021.e06091>.
- [76] Rathje, Jackson, M. L.: *Soil chemical analysis*. Verlag: Prentice Hall, Inc., Englewood Cliffs, NJ. 1958, 498 S. DM 39.40, *Zeitschrift Für Pflanzenernährung, Düngung, Bodenkd.* 85 (1959) 251–252. <https://doi.org/10.1002/JPLN.19590850311>.
- [77] J.W. O'dell, *METHOD 350.1 DETERMINATION OF AMMONIA NITROGEN BY SEMI-AUTOMATED COLORIMETRY ENVIRONMENTAL MONITORING SYSTEMS LABORATORY OFFICE OF RESEARCH AND DEVELOPMENT U*, 1993.
- [78] A.A. Hassan, *Production of vegetable crops*. Book ISSN 7391 710 pages., 2011.
- [79] A. Helaly, A.E. Ashmawi, A.A. Mohammed, M.T. El- Abd, A.S. Nofal, Effect of soil application of nano NPK fertilizers on growth, productivity and quality of Lettuce (*Lactuca sativa*), *Al-Azhar J. Agric. Res.* 46 (2021) 91–100. <https://doi.org/10.21608/ajar.2021.218559>.
- [80] F. Mariotti, D. Tomé, P.P. Mirand, Converting Nitrogen into Protein—Beyond 6.25 and Jones' Factors, <https://doi.org/10.1080/10408390701279749>. 48 (2008) 177–184. <https://doi.org/10.1080/10408390701279749>.
- [81] P. Kumar, R.L. Eriksen, I. Simko, A. Shi, B. Mou, Insights into nitrogen metabolism in the wild and cultivated lettuce as revealed by transcriptome and weighted gene co-expression network analysis, *Sci. Rep.* 12 (2022). <https://doi.org/10.1038/s41598-022-13954-z>.
- [82] E. Ghadamnan, S.R. Nabavi, M. Abbasi, Nano LTA Zeolite in Water Softening Process: Synthesis, Characterization, Kinetic studies and process optimization by Response Surface Methodology (RSM), *J. Water Environ. Nanotechnol.* 4 (2019) 119–138. <https://doi.org/10.22090/jwent.2019.02.004>.
- [83] E.P. Ng, J.M. Goupil, A. Vicente, C. Fernandez, R. Retoux, V. Valtchev, S. Mintova, Nucleation and crystal growth features of EMT-type zeolite synthesized from an organic-template-free system, *Chem. Mater.* 24 (2012) 4758–4765. [https://doi.org/10.1021/CM3035455/SUPPL\\_FILE/CM3035455\\_SI\\_001.PDF](https://doi.org/10.1021/CM3035455/SUPPL_FILE/CM3035455_SI_001.PDF).
- [84] S. Inagaki, K. Thomas, V. Ruaux, G. Clet, T. Wakihara, S. Shinoda, S. Okamura, Y. Kubota, V. Valtchev, Crystal growth kinetics as a tool for controlling the catalytic performance of a FAU-type basic catalyst, *ACS Catal.* 4 (2014) 2333–2341. [https://doi.org/10.1021/CS500153E/SUPPL\\_FILE/CS500153E\\_SI\\_001.PDF](https://doi.org/10.1021/CS500153E/SUPPL_FILE/CS500153E_SI_001.PDF).
- [85] S. Bohra, D. Kundu, M.K. Naskar, One-pot synthesis of NaA and NaP zeolite powders using agro-waste material and other low cost organic-free precursors, *Ceram. Int.* 40 (2014) 1229–1234. <https://doi.org/10.1016/J.CERAMINT.2013.06.001>.
- [86] C.S. Cundy, P.A. Cox, The hydrothermal synthesis of zeolites: History and development from the earliest days to the present time, *Chem. Rev.* 103 (2003) 663–701. [https://doi.org/10.1021/CR020060I/ASSET/CR020060I.FP.PNG\\_V03](https://doi.org/10.1021/CR020060I/ASSET/CR020060I.FP.PNG_V03).
- [87] T. Hu, W. Gao, X. Liu, Y. Zhang, C. Meng, Synthesis of zeolites Na-A and Na-X from tablet compressed and calcinated coal fly ash, *R. Soc. Open Sci.* 4 (2017) 170921. <https://doi.org/10.1098/rsos.170921>.
- [88] R.K. Parsapur, P. Selvam, Rational design, synthesis, characterization and catalytic properties of high-quality low-silica hierarchical FAU- and LTA-type zeolites, *Sci. Rep.* 8 (2018) 16291. <https://doi.org/10.1038/s41598-018-34479-4>.
- [89] Z. Liu, J. Zhu, T. Wakihara, T. Okubo, Ultrafast synthesis of zeolites: breakthrough, progress and perspective, *Inorg.*

- Chem. Front. 6 (2019) 14–31. <https://doi.org/10.1039/C8QI00939B>.
- [90] N. Sapawe, A.A. Jalil, S. Triwahyono, M.I.A. Shah, R. Jusoh, N.F.M. Salleh, B.H. Hameed, A.H. Karim, Cost-effective microwave rapid synthesis of zeolite NaA for removal of methylene blue, *Chem. Eng. J.* 229 (2013) 388–398. <https://doi.org/10.1016/J.CEJ.2013.06.005>.
- [91] I. Kannagara, Y. Jayawardhana, E. Munasinghe, A. Rajapakse, A. Bandara, R. Weerasooriya, L. Jayarathna, Synthesis and characterization of nano zeolite-A with aid of sodium dodecyl sulfate (SDS) as particle size-controlling agent, *Colloids Surfaces A Physicochem. Eng. Asp.* 589 (2020) 124427. <https://doi.org/10.1016/j.colsurfa.2020.124427>.
- [92] A. Khaleque, M.M. Alam, M. Hoque, S. Mondal, J. Bin Haider, B. Xu, M.A.H. Johir, A.K. Karmakar, J.L. Zhou, M.B. Ahmed, M.A. Moni, Zeolite synthesis from low-cost materials and environmental applications: A review, *Environ. Adv.* 2 (2020) 100019. <https://doi.org/10.1016/j.envadv.2020.100019>.
- [93] T. Derbe, S. Temesgen, M. Bitew, A Short Review on Synthesis, Characterization, and Applications of Zeolites, *Adv. Mater. Sci. Eng.* 2021 (2021) 1–17. <https://doi.org/10.1155/2021/6637898>.
- [94] M. Verma, G. Kaur, WITHDRAWN: A mini review on zeolite, *Mater. Today Proc.* (2021). <https://doi.org/10.1016/j.matpr.2021.04.271>.
- [95] A. Julbe, M. Drobek, Zeolite A Type, in: *Encycl. Membr.*, Springer Berlin Heidelberg, Berlin, Heidelberg, 2016: pp. 2055–2056. [https://doi.org/10.1007/978-3-662-44324-8\\_604](https://doi.org/10.1007/978-3-662-44324-8_604).
- [96] E. Nyankson, J.K. Efavi, A. Yaya, G. Manu, K. Asare, J. Daafuor, R.Y. Abrokwah, Synthesis and characterisation of zeolite-A and Zn-exchanged zeolite-A based on natural aluminosilicates and their potential applications, *Cogent Eng.* 5 (2018) 1440480. <https://doi.org/10.1080/23311916.2018.1440480>.
- [97] Y. Huang, J. Yao, X. Zhang, C. (Charlie) Kong, H. Chen, D. Liu, M. Tsapatsis, M.R. Hill, A.J. Hill, H. Wang, Role of ethanol in sodalite crystallization in an ethanol–Na<sub>2</sub>O–Al<sub>2</sub>O<sub>3</sub>–SiO<sub>2</sub>–H<sub>2</sub>O system, *CrystEngComm.* 13 (2011) 4714. <https://doi.org/10.1039/c1ce05194f>.
- [98] R. Pimsen, P. Porrawatkul, P. Nuengmatcha, S. Ramasoot, S. Chanthai, Efficiency enhancement of slow release of fertilizer using nanozeolite–chitosan/sago starch-based biopolymer composite, *J. Coatings Technol. Res.* 18 (2021) 1321–1332. <https://doi.org/10.1007/s11998-021-00495-9>.
- [99] P. Wang, Q. Sun, Synthesis and characterisation of zeolite LTA with sheet structure, *Micro Nano Lett.* 15 (2020) 433–436. <https://doi.org/10.1049/mnl.2019.0793>.
- [100] J. Shen, Q. Sun, J. Cao, P. Wang, W. Jia, S. Wang, P. Zhao, Z. Wang, A lamellar structure zeolite LTA for CO<sub>2</sub> capture, *New J. Chem.* 46 (2022) 6720–6728. <https://doi.org/10.1039/D1NJ05908D>.
- [101] A. Julbe, M. Drobek, Zeolite X: Type, in: *Encycl. Membr.*, Springer Berlin Heidelberg, Berlin, Heidelberg, 2014: pp. 1–2. [https://doi.org/10.1007/978-3-642-40872-4\\_607-1](https://doi.org/10.1007/978-3-642-40872-4_607-1).
- [102] A. Julbe, M. Drobek, Zeolite Y Type, in: *Encycl. Membr.*, Springer Berlin Heidelberg, Berlin, Heidelberg, 2016: pp. 2060–2061. [https://doi.org/10.1007/978-3-662-44324-8\\_608](https://doi.org/10.1007/978-3-662-44324-8_608).
- [103] A. Julbe, M. Drobek, Zeolite T Type, in: *Encycl. Membr.*, Springer Berlin Heidelberg, Berlin, Heidelberg, 2016: pp. 2058–2059. [https://doi.org/10.1007/978-3-662-44324-8\\_606](https://doi.org/10.1007/978-3-662-44324-8_606).
- [104] A.S. Giroto, S.F. do Valle, G.G.F. Guimarães, N.D. Jablonowski, C. Ribeiro, L.H.C. Mattoso, Different Zn loading in Urea–Formaldehyde influences the N controlled release by structure modification, *Sci. Rep.* 11 (2021) 7621. <https://doi.org/10.1038/s41598-021-87112-2>.
- [105] O. Onija, G. Borodi, I. Kacso, M. Pop, D. Dadarlat, I. Bratu, N. Jumate, Preparation And Characterization Of Urea-Oxalic Acid Solid Form, *AIP Conf. Proc.* 1425 (2012) 35–38. <https://doi.org/10.1063/1.3681960>.
- [106] M. Firdaus, M. Prameswari, Synthesis of 2,2,4-Trimethyl-2,3-dihydro-1H-1,5-benzodiazepine using Treated Natural Zeolite Catalyst, *Bull. Chem. React. Eng. Catal.* 14 (2019) 9–16. <https://doi.org/10.9767/brec.14.1.2222.9-16>.
- [107] R. Naikoo, S. Bhat, M. Mir, R. Tomar, W. Khanday, P. Dipak, D. Tiwari, Polypyrrole and its composites with various cation exchanged forms of zeolite X and their role in sensitive detection of carbon monoxide, *RSC Adv.* 6 (2016) 99202–99210. <https://doi.org/10.1039/c6ra19708f>.
- [108] J. Madhu, A. Santhanam, M. Natarajan, D. Velauthapillai, CO<sub>2</sub> adsorption performance of template free zeolite A and X synthesized from rice husk ash as silicon source, *RSC Adv.* 12 (2022) 23221–23239. <https://doi.org/10.1039/D2RA04052B>.
- [109] J. Madhu, V. Madurai Ramakrishnan, A. Santhanam, M. Natarajan, B. Palanisamy, D. Velauthapillai, N.T. Lan Chi, A. Pugazhendhi, Comparison of three different structures of zeolites prepared by template-free hydrothermal method and its CO<sub>2</sub> adsorption properties, *Environ. Res.* 214 (2022) 113949. <https://doi.org/10.1016/J.ENVRES.2022.113949>.